

Photoemission Evidence for a Remnant Fermi Surface and d -Wave-Like Dispersion in Insulating $\text{Ca}_2\text{CuO}_2\text{Cl}_2$

F. Ronning⁽¹⁾, C. Kim⁽¹⁾, D.L. Feng⁽¹⁾, D.S. Marshall⁽¹⁾, A.G. Loeser⁽¹⁾, L.L. Miller⁽²⁾, J.N. Eckstein⁽³⁾,
I. Bozovic⁽³⁾, Z.-X. Shen⁽¹⁾

⁽¹⁾ *Department of Physics and Stanford Synchrotron Radiation Laboratory, Stanford University, Stanford, CA 94305-4045*

⁽²⁾ *Department of Physics, Iowa State University, Ames, IA 50011*

⁽³⁾ *Ginzton Research Center, Varian Associates, Palo Alto, CA 94304*

An angle resolved photoemission study on $\text{Ca}_2\text{CuO}_2\text{Cl}_2$, a parent compound of high T_c superconductors is reported. Analysis of the electron occupation probability, $n(k)$, from the spectra shows a steep drop in spectral intensity across a contour that is close to the Fermi surface predicted by the band calculation. This analysis reveals a Fermi surface remnant even though $\text{Ca}_2\text{CuO}_2\text{Cl}_2$ is a Mott insulator. The lowest energy peak exhibits a dispersion with approximately the $|\cos(k_x a) - \cos(k_y a)|$ form along this remnant Fermi surface. Together with the data from Dy doped $\text{Bi}_2\text{Sr}_2\text{CaCu}_2\text{O}_{8+\delta}$ these results suggest that this d -wave like dispersion of the insulator is the underlying reason for the pseudo gap in the underdoped regime.

I. INTRODUCTION

Introduction: A consensus on the $d_{x^2-y^2}$ pairing state and the basic phenomenology of the anisotropic normal state gap (pseudo gap) in high- T_c superconductivity has been established [1], partially on the basis of angle-resolved photoemission spectroscopy (ARPES) experiments [2] [3] [4] [5], in which two energy scales have been identified in the pseudo gap, a leading-edge shift of 20-25 meV and a high-energy hump at 100-200 meV. [4] Both of these features have an angular dependence consistent with a d -wave gap. For simplicity in the discussion below, we refer to these as low- and high-energy pseudo gaps, respectively, in analogy to the analysis of other data. [6] The evolution of these two pseudo gaps as a function of doping are correlated [7], but the microscopic origin of the pseudo gap and its doping dependence are still unestablished. Theoretical ideas of the pseudo gap range from pre-formed pairs or pair fluctuation [8] and damped spin density wave (SDW) [9] to the evidence of the resonating valence bond (RVB) singlet formation and spin-charge separation [10] [11] [12].

To further differentiate these ideas, it is important to understand how the pseudo gap evolves as the doping is lowered and the system becomes an insulator. We present experimental data from the insulating analog of the superconductor $\text{La}_{2-x}\text{Sr}_x\text{CuO}_4$, $\text{Ca}_2\text{CuO}_2\text{Cl}_2$ which suggest that the high energy pseudo gap is a remnant property of the insulator that evolves continuously with doping, as first pointed out by Laughlin. [12] The Compound $\text{Ca}_2\text{CuO}_2\text{Cl}_2$, a half-filled Mott insulator, has the crystal structure of La_2CuO_4 [13] and it can be doped by replacing Ca with Na or K to become a high-temperature superconductor. [14] As with the case of $\text{Sr}_2\text{CuO}_2\text{Cl}_2$, $\text{Ca}_2\text{CuO}_2\text{Cl}_2$ has a much better surface property than La_2CuO_4 and thus is better suited for ARPES experiments. [15] Although the data from $\text{Ca}_2\text{CuO}_2\text{Cl}_2$ are consistent with earlier results from $\text{Sr}_2\text{CuO}_2\text{Cl}_2$, [16] [17] [18]

the improved spectral quality obtainable from this material allows us to establish that: (I) The Fermi surface, which is destroyed by the strong Coulomb interactions, left a remnant in this insulator with a volume and shape similar to what one expects if the strong electron correlation in this system is turned off; (II) The strong correlation effect deforms this otherwise iso-energetic contour (the non-interacting Fermi surface) into a form that matches the $|\cos(k_x a) - \cos(k_y a)|$ function very well, but with a very high energy scale of 320 meV. Thus, a d -wave like dispersive behavior exists even in the insulator.

Comparison with data from underdoped $\text{Bi}_2\text{Sr}_2\text{CaCu}_2\text{O}_{8+\delta}$ (Bi2212) with T_c 's of 0, 25 and 65 K indicates that the high energy d -wave like pseudo gap in the underdoped regime originates from the d -wave like dispersion in the insulator. Once doped to a metal, the chemical potential drops to the maximum of this d -wave like function, but the dispersion relation retains its qualitative shape, albeit the magnitude decreases with doping. Thus, only the states near the d -wave node touch the Fermi level and form small segments of the Fermi surface, with the rest of Fermi surface gapped. In this way, the d -wave high energy pseudo gap in the underdoped regime is naturally connected to the properties of the insulator. Since the high energy pseudo gap correlates with the low energy pseudo gap which is likely to be related to superconductivity [3] [4] [5] [7] [19], it is likely that the same physics that controls the d -wave dispersion in the insulator is responsible for the d -wave like normal state pseudo gap and the superconducting gap in the doped superconductors.

II. METHODOLOGY

To investigate the strong correlation effect, we contrast our experimental data with the conventional results for the case when the correlation effects are neglected. We

can obtain the occupation probability, $n(k)$, by integrating $A(k,\omega)$ obtained by ARPES, over energy. [20] Experimentally $A(k,\omega)$ can not be integrated over all energies due to contributions from secondary electrons and other electronic states. Instead an energy window for integration must be chosen, and the resulting quantity we define as the *relative* $n(k)$. Fortunately, the features we are interested in are clearly distinguishable from any other contributions. We note that $n(k)$ is a ground state property, and hence is different from the integration of the single-particle spectral weight, $A(k,\omega)$, over energy. However, under the sudden approximation integration of $A(k,\omega)$ as measured by ARPES gives $n(k)$. [20] We then use the drop of the relative $n(k)$ to determine the Fermi surface as illustrated in Fig. 1. For a metal with non-interacting electrons, the electron states are filled up to the Fermi momentum, k_F , and the $n(k)$ shows a sudden drop (Fig. 1A). As more electrons are added, the electron states are eventually filled and the system becomes an insulator with no drop in $n(k)$ (Fig. 1B). Therefore, the drop in $n(k)$ characterizes the Fermi surface of a metal with non-interacting electrons. When correlation increases, $n(k)$ begins to deform (Fig. 1C), although there is still some discontinuity at k_F when the correlation is moderate. Note that the electrons that used to occupy states below k_F have moved to the states that were unoccupied. For a non-Fermi liquid with very strong correlation, $n(k)$ drops smoothly without a discontinuity (panel D). Several theoretical calculations using very different models have found that $n(k)$ of the interacting system mimics that of the non-interacting system, even when the material is fully gapped [21] [22] [23] [24]. Hence we can recover the remnant of a Fermi surface or an underlying Fermi surface by following the contour of steepest descent of $n(k)$ even when correlation is strong enough that the system becomes a Mott insulator. [25] The volume obtained by this procedure is consistent with half-filling as expected in a Mott insulator.

We apply this method to determine the Fermi level crossing of a real system. The traditional way (Fig. 2A) is shown for the ARPES spectra on the $(0,0)$ to (π,π) cut taken from Bi2212 which is metallic. As we move from $(0,0)$ toward (π,π) , the peak disperses to the Fermi level, E_F . As the peak reaches E_F and passes it, it begins to lose spectral weight (this again is k_F). Alternatively, we simply integrate the spectral function from 0.6 eV to -0.1 eV relative to the E_F , and the resulting relative $n(k)$ is plotted in Fig. 2C. We can now define k_F as the point of steepest descent in the relative $n(k)$. The same conclusion can be drawn here independent of the method we use. Note that the $n(k)$ also drops as we approach $(0,0)$; this is a photoemission artifact, because the photoemission cross-section of the $d_{x^2-y^2}$ orbital vanishes due to symmetry.

We can show that the $n(k)$ procedure is still valid for strongly correlated systems with gapped Fermi sur-

face by presenting ARPES spectra on ferromagnetic $\text{La}_{3-x}\text{Sr}_x\text{Mn}_2\text{O}_7$ on the $(\pi,0)$ to (π,π) cut (Fig. 2B). [26] It shows a dispersive feature initially moving toward E_F and then pulling slightly back away from E_F around $(\pi,0.27\pi)$, but never reaching the E_F . However, the feature suddenly loses its spectral weight when it crosses $(\pi,0.27\pi)$ as if it crosses the Fermi surface as shown in panel D. Furthermore, the Fermi surface determined by a local density approximation calculation coincides with the Fermi surface determined by the $n(k)$ despite the spectra of this ferromagnetic metallic state material having a significant gap. Thus, the underlying Fermi surface can survive a strong interaction, and the $n(k)$ method is effective in identifying it even when the peak does not disperse across E_F .

III. EXPERIMENTAL RESULTS

The low-energy feature along the $(0,0)$ to (π,π) cut on $\text{Ca}_2\text{CuO}_2\text{Cl}_2$ (Fig. 3A) has the same origin as the low energy peak seen in Bi2212, the Zhang-Rice singlet on the CuO_2 plane. As k increases from $(0,0)$ toward (π,π) , the peak moves to lower energy and subsequently pulls back to higher energy as it crosses $(\pi/2,\pi/2)$. Its spectral weight increases as it moves away from the $(0,0)$ point for the reason described earlier, and then drops as it crosses $(0.43\pi,0.43\pi)$. These changes along the $(0,0)$ to (π,π) cut are consistent with the earlier reports on $\text{Sr}_2\text{CuO}_2\text{Cl}_2$. [16] [17] [18] Similar to the drop of $n(k)$ across the Fermi surface seen in Bi2212, $\text{Ca}_2\text{CuO}_2\text{Cl}_2$ also shows that the intensity of the peak $n(k)$ drops as if there is a crossing of E_F even though the material is an insulator. The intensity along the $(0,0)$ to $(\pi,0)$ cut (Fig. 3B) goes through a maximum around $(2\pi/3,0)$ as in $\text{Sr}_2\text{CuO}_2\text{Cl}_2$. This behavior is also seen in superconducting cuprates. [27] Earlier works on $\text{Sr}_2\text{CuO}_2\text{Cl}_2$ show the spectral weight along the $(\pi,0)$ to (π,π) cut is strongly suppressed. However, for $\text{Ca}_2\text{CuO}_2\text{Cl}_2$, the improved spectral quality allows us to clearly observe the spectral weight drop along the $(\pi,0)$ to (π,π) cut (Fig. 3C). [28] Note that the spectral weight drops as we move toward the (π,π) point, which we attribute to the crossing of a remnant Fermi surface. We also show another cut (Fig. 3D) which exhibits essentially the same behavior. The relative $n(k)$ s of the cuts are summarized in Fig. 3E in arbitrary units. The relative $n(k)$ here and in fig. 4 were obtained by integrating from 0.5 eV to -0.2 eV relative to the peak position at $(\pi/2,\pi/2)$. All of the $n(k)$ s show a drop (after the maximum) as we cross the remnant Fermi surface. Here we emphasize that we are using the same method as we do for metals, where the identification of a Fermi surface is convincing.

The remnant Fermi surface can be identified in the contour plot of $n(k)$ of $\text{Ca}_2\text{CuO}_2\text{Cl}_2$ (Fig. 4A). The little crosses in the figure denote the k -space points where spec-

tra were taken. The data points here and in Fig. 4C have been reflected about the line $k_y=k_x$ to better illustrate the remnant Fermi surface. Again, it should be emphasized that the suppressed $n(k)$ near $(0,0)$ comes from the vanishing photoemission cross section due to the $d_{x^2-y^2}$ orbital symmetry rather than a remnant Fermi surface crossing. For the same reason, the photon polarization suppresses the overall spectral weight along the $(0,0)$ to (π, π) line as compared with the $(0,0)$ to $(\pi, 0)$ line, with a monotonic change between the two directions. In fig. 4B we present the relative $n(k)$ of an optimally doped Bi2212 sample in the normal state. In this case the identification of the Fermi surface is unambiguous, but the same matrix element effects that were seen in the insulator can be seen in the metallic sample as well. However, for both samples, the drop in $n(k)$ near the diagonal line connecting $(\pi, 0)$ and $(0, \pi)$ can not be explained by the photoemission cross section. In the metallic case, the Fermi surface is clearly identified (the white-hashed region in Fig. 4B). For the insulator, the drop is approximately where band theory predicts the Fermi surface. [29] Therefore, we attribute the behavior in the insulator to a remnant of the Fermi surface that existed in the metal. The similarity of the results in the insulator and the metal makes the identification of the remnant Fermi surface unambiguous. The white hashed area in Fig. 4A represents the area where the remnant Fermi surface may reside as determined by the relative $n(k)$. Although there is some uncertainty in the detailed shape of this remnant Fermi surface, this does not affect the discussion and the conclusions drawn below. The relative $n(k)$ we presented is a very robust feature. In metallic samples with partially gapped Fermi surfaces, underlying Fermi surfaces have also been identified in the gapped region. [26] [30] This effect is similar to what we report here in the insulator. The remnant Fermi surface in the underdoped Bi2212 was also identified at similar locations to the $n(k)$ drop in these materials with a different criteria of minimum gap locus. [30] Calculations also show the Fermi surface defined by $n(k)$ is robust in the presence of strong correlation. [21] [23] [24] Given that there is a remnant Fermi Surface as shown by the white hashed lines in Fig. 4, A and C, the observed energy dispersion along this line has to stem from the strong electron correlation. In other words, the electron correlation disperses the otherwise iso-energetic contour of the remnant Fermi surface. This dispersion is consistent with the non-trivial d -wave $|\cos(k_x a) - \cos(k_y a)|$ form. [10] [11] [12] These results also support our identification of the remnant Fermi surface in a Mott insulator.

Fig. 4C plots the energy contour of the peak position of the lowest energy feature of $\text{Ca}_2\text{CuO}_2\text{Cl}_2$ referenced to the energy of $(\pi/2, \pi/2)$ peak. The hashed area indicates the remnant Fermi surface determined in fig. 4A. The 'Fermi surface' is no longer a constant energy contour as it would be in the non-interacting case. Instead

it disperses as much as the total dispersion width of the system. In Fig. 4D we plot the dispersion at different points on the remnant Fermi surface referenced to the lowest energy state at $(\pi/2, \pi/2)$. The dispersion of the peaks along the Fermi surface is plotted against $|\cos(k_x a) - \cos(k_y a)|$. The straight line shows the d -wave dispersion function at the 'Fermi surface' with a d -wave energy gap. The figure in the inset presents the same data in a more illustrative fashion. On a line drawn from the center of the Brillouin zone to any point either experimental (blue) or theoretical (red), the distance from this point to the intersection of the line with the anti-ferromagnetic Brillouin zone boundary gives the value of the 'gap' at the k -point of interest. The red line is for a d -wave dispersion along $(\pi, 0)$ to $(0, \pi)$. The good agreement [31] is achieved without the need for free parameters. This d -wave like dispersion can only be attributed to the many-body effect. The relative energy difference between the energy at $(\pi/2, \pi/2)$ and $(\pi, 0)$ has been referred to as a gap [12], which we follow.

This gap differs from the usual optical Mott gap (Fig. 5) and may correspond to the momentum dependent gap once the system is doped. This gap monotonically increases when we move away from $(\pi/2, \pi/2)$ as also reported earlier. [16] As well as summarizing the data presented, Fig. 5 also shows the intriguing similarity between the data from the insulator and a slightly overdoped d -wave superconductor (Bi2212), and thus gives the reason for comparing the dispersion along the remnant Fermi surface with the $|\cos(k_x a) - \cos(k_y a)|$ form. In the superconducting case, $n(k)$ helps determine the Fermi surface. The anisotropic gapping of this surface below T_c reveals the d -wave nature of the gap. In the insulator, $n(k)$ helps determine the remnant Fermi surface. The k -dependent modulation along this surface reveals the d -wave like dispersion. Whether this similarity between the insulator and the doped superconductor is a reflection of some underlying symmetry principle is a question which needs to be investigated. [32]

The above analysis is possible only because we now observe the remnant Fermi surface. Although the dispersion for $\text{Sr}_2\text{CuO}_2\text{Cl}_2$ was similar to the present case, the earlier results did not address the issue of a remnant Fermi surface because the smaller photoemission cross section along the $(\pi, 0)$ to (π, π) cut prevented this identification. Therefore the analysis shown above was not possible. With only the energy contour information (such as in Fig 4C), it is plausible to think that the Fermi surface evolves to a small circle around the $(\pi/2, \pi/2)$ point. [33] However, with the favorable photoemission cross section, the results from $\text{Ca}_2\text{CuO}_2\text{Cl}_2$ show that the Fermi surface leaves a clear remnant, although it may be broadened and weakened. Therefore, the energy dispersion along the original Fermi surface of a non-interacting system is due to the opening of an anisotropic 'gap' along the same remnant Fermi surface.

The same analysis is shown in Fig. 6 for Bi2212 with different Dy dopings together with $\text{Ca}_2\text{CuO}_2\text{Cl}_2$ results. The corresponding doping level and T_c as a function of Dy concentration are also shown. The energy for $\text{Ca}_2\text{CuO}_2\text{Cl}_2$ is referenced to the peak position at $(\pi/2, \pi/2)$ and that for Dy doped Bi2212 is to E_F . However, the two energies essentially refer to the same energy since the peak on the $(0,0)$ to (π, π) cut for all Bi2212 samples reaches the Fermi level. Note that the gaps for Dy doped Bi2212 data also follow a function that is qualitatively similar to the d -wave function with reduced gap sizes as shown with the $(\pi, 0)$ spectra in Fig. 6B. This result suggests that the d -wave gap originating in the insulator continuously evolves with doping, but retains its anisotropy as a function of momentum and that the high energy pseudo gap in the underdoped regime is the same gap as the d -wave gap seen in the insulator as discussed above. Of course, the high energy pseudo gap in the underdoped regime is smaller than the gap in the insulator. In a sense, the doped regime is a diluted version of the insulator, with the gap getting smaller with increasing doping. The two extremes of this evolution are illustrated in the quasiparticle dispersions shown in Fig. 5. The insulator shows a large d -wave like dispersion along the remnant Fermi surface. In the overdoped case, no gap is seen in the normal state along an almost identical curve in k -space; however, a d -wave gap is observed in the superconducting state. Although their sizes vary, the d -wave superconducting gap, and the d -wave 'gap' of the insulator have the same non-trivial form, and are thus likely to stem from the same underlying mechanism.

IV. DISCUSSION

We do not know the full implications of the data we report, but can offer the following possibilities. First, we compare the experimental dispersion with a simple spin-density wave picture. Starting with the Hubbard model

$$H = \sum_{k\sigma} \epsilon_k c^\dagger_{k\sigma} c_{k\sigma} + U \sum_i n_{i\uparrow} n_{i\downarrow}$$

with

$$\epsilon_k = -2t(\cos(k_x a) + \cos(k_y a)) - 4t'(\cos(k_x a)\cos(k_y a)) - 2t''(\cos(2k_x a) + \cos(2k_y a))$$

and adding a SDW picture, the following dispersion relation will be found

$$E_{k\pm} \approx -4t'(\cos(k_x a)\cos(k_y a)) - 2t''(\cos(2k_x a) + \cos(2k_y a)) \pm [U/2 + J(\cos(k_x a) + \cos(k_y a))]^2$$

with $J=t^2/U$. With realistic values for t' and t'' , and an experimental value for J of -0.12 eV, 0.08 eV, and 0.125 eV respectively, [18] we find that the experimental dispersion deviates significantly from this mean field result giving a bandwidth of 1.1 eV. It is crucial to note the observed isotropic dispersion around the $(\pi/2, \pi/2)$ point, with almost identical dispersions from $(\pi/2, \pi/2)$

to $(0,0)$ and from $(\pi/2, \pi/2)$ to $(\pi, 0)$. This result is unlikely to be a coincidence of the parameters t' , t'' , and J as suggested by the SDW picture above.

We now compare the data with numerical calculations that, unlike the mean field SDW picture, appropriately accounts for the dynamics. Being mainly concerned with the dispersion relation, we concentrate our discussion on the t - J model as more extensive literature exists and as J can be independently measured. [24] Qualitatively, the same conclusion is expected for the Hubbard model [34], which has the added advantage of yielding $n(k)$, but has more uncertainty in the parameter U . Although the t - J model correctly predicts [24] the dispersion along $(0,0)$ to $(\pi/2, \pi/2)$ quantitatively [16], with the band width along this direction solely determined by J , it incorrectly predicts the energy of $(\pi, 0)$ to be nearly degenerate to $(\pi/2, \pi/2)$. This is a serious deficiency of the t - J model, because the evolution of the $(\pi, 0)$ feature is crucial to understand the d -wave-like pseudo gap. The inclusion of the next nearest neighbor hoppings of t' and t'' can resolve this problem. [34] [35] [36] In fact, the t - t' - t'' - J model can account for both the dispersion and lineshape evolution over all doping levels, which is a remarkable success of this model. [18] [35] With a J/t ratio in the realistic range of 0.2 to 0.6, the t - t' - t'' - J model shows that the dispersion from $(\pi/2, \pi/2)$ to $(0,0)$ and to $(\pi, 0)$ are equal and scaled by J . [37] This result supports the notion that the isotropic dispersion is controlled by a single parameter, J , as stressed by Laughlin. [12]

The above discussion indicates that we have a model, when solved by Monte Carlo or exact diagonalization, that can account for the data, but what does the data fitting the non-trivial $|\cos(k_x a) - \cos(k_y a)|$ function so well mean? As pointed out [18], the key to the inclusion of t' and t'' is that the additional hole mobility destabilizes the one-hole Néel state with the hole at $(\pi, 0)$ and makes the system with one-hole move closer to a spin liquid state rather than to a Néel state that is stable in the t - J model. This point is relevant to some early literature of the resonating valence bond (RVB) state [38] [39]. Anderson conjectured that the ground state of the insulator at half filling is a RVB spin liquid state. [38] This idea was extended in the context of a mean field approach to the t - J model that yields a d -wave RVB or flux phase solution. [10] The mean-field solution also predicts a phase diagram similar to what is now known about the cuprates, with the d -wave like spin gap in the underdoped regime being the most successful example. The problem with the mean-field solution of the t - J model is that it does not agree with exact numerical calculation results [24], and the half-filled state was found by neutron scattering to have long range order. [40] If these numerical calculations are right then the d -wave RVB is not the right solution of the t - J model. However, the d -wave RVB like state may still be a reasonable way to think about the experimental data that describes the situation of the spin

state near a hole. [41] It is just that one has to start with a model where the single hole Néel state is destabilized, as in the t-t'-t''-J model. We leave this open question as a challenge to theory.

The presence of *d*-wave like dispersion along the remnant Fermi surface shows that the high energy pseudo gap is a remnant of the *d*-wave 'gap' seen in the insulator. The details of the evolution of this gap, and its connection to the low energy pseudo gap (which is likely due to pairing fluctuations) as well as the superconducting gap is unclear at the moment. However, we believe that there has to be a connection between these gaps of the similar $|\cos(k_x a) - \cos(k_y a)|$ form, as their presence is correlated with each other. [7]

-
- [1] B.G. Levi, *Phys. Today*, **46**(5), 17 (1993); *ibid.*, **49**(1), 19 (1996); *ibid.*, **49**(6), 17 (1996).
- [2] Z.-X. Shen *et al.*, *Phys. Rev. Lett.* **70**, 1553 (1993)
- [3] A.G. Loeser *et al.*, *Science*, **273**, 325 (1996)
- [4] D.S. Marshall *et al.*, *Phys. Rev. Lett.* **76**, 4841 (1996)
- [5] H. Ding *et al.*, *Nature*, **382**, 51 (1996)
- [6] B. Battlog and V.J. Emery, *ibid.*, **382**, 20 (1996).
- [7] P.J. White *et al.*, *Phys. Rev. B* **54**, R15669 (1996)
- [8] S.A. Kivelson and V.J. Emery, *Nature*, **374**, 434 (1995) C.A.R. de sa Melo, M Randeria, J. Engelbrecht, *Phys. Rev. Lett.* **71**, 3202 (1993); N Trivedi and M. Randeria, *ibid.* **75**, 312 (1995) S. Doniach and M. Inui, *Phys. Rev. B* **41**, 6668 (1990). A.J. Millis, L.B. Ioffe, and H. Monien, *J. Phys. Chem. Solids* **56**, 1641 (1995). B. Janko, J. Maly, and K. Levin, *Phys. Rev. B* **56**, R11407 (1997). Y. J. Uemura, *et al.*, *Phys. Rev. Lett.* **62**, 2317 (1989); Y. J. Uemura, *High-T_c Superconductivity and the C₆₀ family*, edited by Sungi Feng and Hai-Cang Ren, Gordon and Breach Publishers (1994).
- [9] J. Schmalian, D. Pines, and B. Stojkovic, *Phys. Rev. Lett.* **80**, 3839 (1998); J. Schmalian, D. Pines, and B. Stojkovic, <http://xxx.lanl.gov/abs/cond-mat/9804129>. A.V. Chubukov and D.K. Morr, <http://xxx.lanl.gov/abs/cond-mat/9806200>.
- [10] T. Tanamoto, K. Kohno, and H. Fukuyama, *J. Phys. Soc. Jpn.* **61**, 1886 (1992); Y. Suzumura, Y. Hasegawa, and H. Fukuyama, *ibid.* **57**, 2768 (1988). G. Kotliar and J. Liu, *Phys. Rev. B* **38**, 5142 (1988)
- [11] X.-G. Wen and P. A. Lee, *Phys. Rev. Lett.* **78**, 4111 (1997).
- [12] R.B. Laughlin, *ibid.* **79**, 1726 (1997).
- [13] L.L. Miller, *et al.*, *Phys. Rev. B* **41**, 1921 (1990).
- [14] Z. Hiroi, *et al.*, *Physica C* **255**, 61 (1995).
- [15] Experiments were performed at beamline V of the Stanford Synchrotron Radiation Laboratory (SSRL). Ca₂CuO₂Cl₂ single crystals[20] were oriented before the experiments by the Laue method and were cleaved in situ by knocking off the top posts that were glued to the samples, giving flat fresh surfaces suitable for ARPES experiments. The base pressure was better than 5x10⁻¹¹ torr. With the photon energies used in the experiments, the total energy resolution was typically 70 meV. The angular resolution was ±1°. The spectra from Ca₂CuO₂Cl₂ reported here were all taken at 100 K with 25.2 eV photons.
- [16] B.O. Wells, *et al.*, *Phys. Rev. Lett.* **74**, 964 (1995)
- [17] S. LaRosa *et al.*, *Phys. Rev. B* **56**, R525 (1997)
- [18] C. Kim, *et al.*, *Phys. Rev. Lett.* **80**, 4245 (1998).
- [19] Z.-X. Shen and J. R. Schrieffer, *ibid.* **78**, 1771 (1997).
- [20] S. Hufner, *Photoelectron spectroscopy : principles and application*, New York : Springer-Verlag, c1995. M. Randeria *et al.*, *Phys. Rev. Lett.* **74**, 4951 (1995).
- [21] W.O. Putikka, M.U. Luchini, and R.R.P. Singh, *ibid.* **81**, 2966 (1998)
- [22] N. Bulut, D.J. Scalapino, and S.R. White, *ibid.* **73**, 748 (1994).
- [23] R. Eder and Y. Ohta, *ibid.* **72**, 2816 (1994)
- [24] E. Dagatto, *Rev. Mod. Phys.* **66**, 763 (1994)
- [25] A key difference between a Mott insulator and a band insulator is that $\sum_k n(k)$ /(Brillouin zone volume) equals 1 for a Mott insulator, and equals 2 for a band insulator.
- [26] D.S. Dessau, *et al.*, *Phys. Rev. Lett.* **81**, 192 (1998).
- [27] D.S. Dessau *et al.*, *Phys. Rev. Lett.* **71**, 2781 (1993)
- [28] As generally found in photoemission experiments, the change of photoemission cross-section for each sample is hard to calculate quantitatively. At the qualitative level, data from Ca₂CuO₂Cl₂ and Sr₂CuO₂Cl₂ are consistent with each other.
- [29] D.L. Novikov, A.J. Freeman, and J.D. Jorgensen, *Phys. Rev. B* **51**, 6675 (1995).
- [30] H. Ding *et al.*, *Phys. Rev. Lett.* **78**, 2628 (1997). J.M. Harris *et al.*, *Phys. Rev. B* **54**, R15665 (1996)
- [31] The details on whether or not the dispersion near the *d*-wave node is a cusp can not yet be addressed due to the broadness of the observed features and the finite resolution. The motivation to compare the data with the *d*-wave function stems from the fact that the insulator is related to a *d*-wave superconductor (and thus a *d*-wave gap) by doping.
- [32] S.C. Zhang, *Science* **275**, 1089 (1997); W. Hanke, unpublished data
- [33] A.V. Chubukov, D.K. Morr, and K.A. Shakhnovich, *Philos. Mag B* **74**, 563 (1996)
- [34] R. Preuss, W. Hanke, W. von der Linden, . *Phys. Rev. Lett.* **75**, 1344 (1995)
- [35] R. Eder *et al.*, *Phys. Rev. B* **55**, R3414 (1997).
- [36] T. Tohyama and S. Maekawa, *ibid.* **49**, 3596 (1994) T. Xiang *et al.*, *ibid* **54**, R12653 (1996) T. Tanamoto *et al.*, *J. Phys. Soc. Jpn.* **62**, 717 (1993) A. Nazarenko *et al.*, *Phys. Rev. B* **51**, 8676 (1995) R. Gooding *et al.*, *ibid* **50**, 12866 (1994) B. Kyung and R.A. Ferrell, *ibid* **54**, 10125 (1996) P.W. Leung *et al.*, *ibid* **56**, 6320 (1997) T.K. Lee *et al.*, *ibid* **55**, 5983 (1997)
- [37] Private Communication with T. Tohyama, S. Maekawa
- [38] P.W. Anderson, *Science* **235**, 1996 (1987).
- [39] S.A. Kivelson, D.S. Rokhsar, and J.P. Sethna, *Phys. Rev. B* **35**, 8865 (1987).
- [40] S. Chakravarty, B.I. Halperin, and D.R. Nelson, *Phys. Rev. Lett.* **60**, 1057 (1988). R.J. Birgeneau, G. Shirane, in *Physical Properties of High Temperature Superconduct-*

tor I, D.M. Ginsberg, Ed.(World Scientific, Singapore, 1989), p151.

- [41] H. Eskes H. Tjeng, G. A. Sawatzky, *Mechanisms of High-Temperature Superconductivity*, H. Kamimuna and A Oshiyama, Eds. (Springer Verlag, Berlin, 1989)
- [42] We would like to acknowledge helpful discussions with R.B. Laughlin, W. Hanke, E. Dagatto, A.J. Millis, N. Nagaosa, P.A. Lee, D. J. Scalapino, B.O. Wells, T. Tohyama, and S. Maekawa. Photoemission experiments were performed at SSRL which is operated by the U.S. Department of Energy office of Basic Energy *Science*, Division of Chemical *Sciences*. The office's division of Material *Science* provided support for this research. The Stanford work was supported also by NSF grant DMR9705210

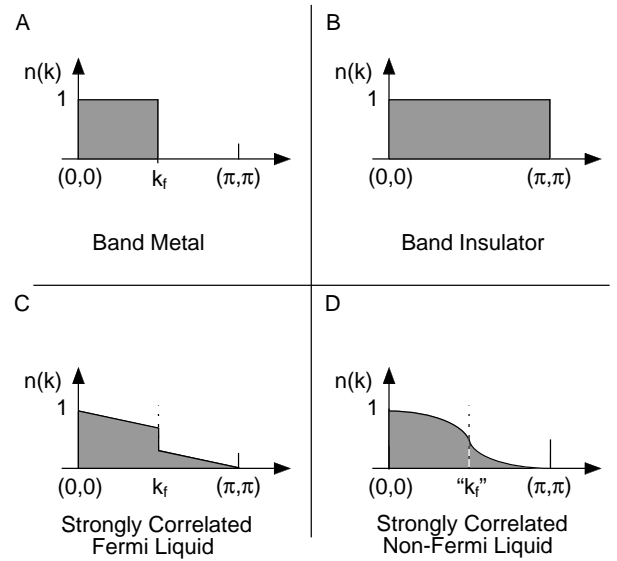


FIG. 1. Illustration of the Fermi surface determination. (A) The case for band metal. Electrons occupy states only up to a certain momentum, showing a sharp drop in $n(k)$. (B) Band insulator case. Electrons occupy all possible states and do not show a drop in $n(k)$. (C) Fermi liquid with electron correlation. Note that electrons that used to occupy the states below k_F have moved above k_F . However, it still shows a discontinuity at k_F . (D) For a strongly correlated non-Fermi liquid $n(k)$ does not show discontinuity, yet there exists $n(k)$ drop showing the remnant Fermi surface.

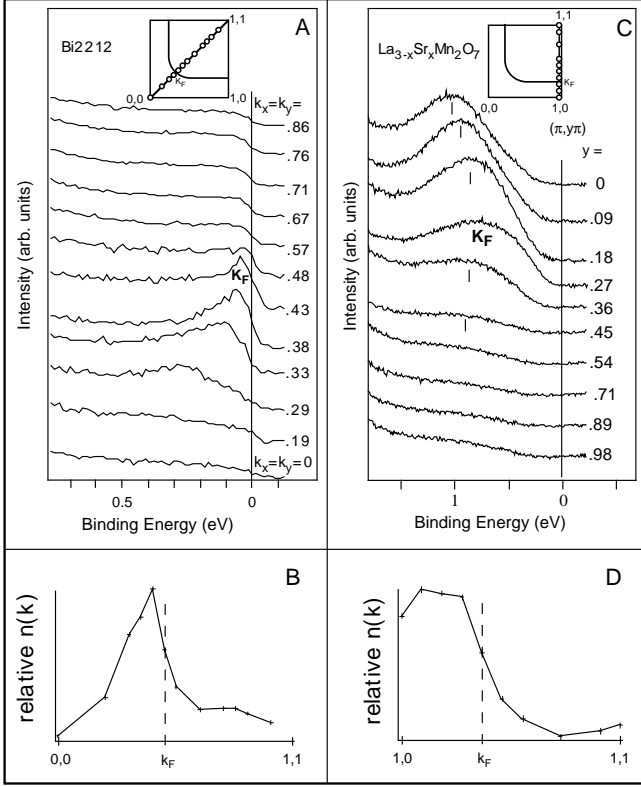


FIG. 2. Application of the method described in Fig.1. (A) Spectra along the $(0,0)$ to (π,π) cut from Bi2212. The peak disperses towards the low energy side and reaches the Fermi level at k_F , $(0.43\pi, 0.43\pi)$. (B) Spectra along the $(\pi,0)$ to (π,π) cut from metallic $\text{La}_{3-x}\text{Sr}_x\text{Mn}_2\text{O}_7$. The peak disperses toward the low energy side, but never reaches the Fermi energy. However, it loses intensity as it crosses the position where the band calculation predicts the Fermi surface, showing an underlying Fermi surface. (C) and (D) plots of the relative $n(k)$ for the data in (A) and (B), respectively, show a sudden drop around k_F , essentially showing the two methods give the same Fermi momentum k_F .

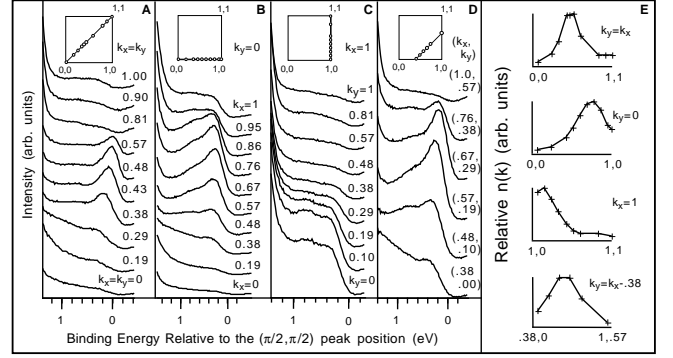


FIG. 3. ARPES Spectra on various cuts from $\text{Ca}_2\text{CuO}_2\text{Cl}_2$ and $n(k)$ plots. The insets and labels show where the spectra were taken in the Brillouin zone. (A) $(0,0)$ to (π,π) cut. The peak disperses towards the low energy side and loses intensity near the $(\pi/2, \pi/2)$ point. (B) $(0,0)$ to $(\pi,0)$ cut. The lowest energy peak shows little dispersion. The spectral weight initially increases and then decreases again after $(0.67\pi, 0)$ as in the $\text{Sr}_2\text{CuO}_2\text{Cl}_2$ case. [17][18] However, note that there is appreciable spectral weight at $(\pi, 0)$ contrary to the $\text{Sr}_2\text{CuO}_2\text{Cl}_2$ case. (C) $(\pi,0)$ to (π,π) cut. The spectral weight drops as we move to (π,π) . (D) Another cut (as marked in the inset) showing the $n(k)$ drop. (E) relative $n(k)$'s constructed from the spectra in panels A-D. The relative increase of spectral weight above 0 is caused by emission from second order light.

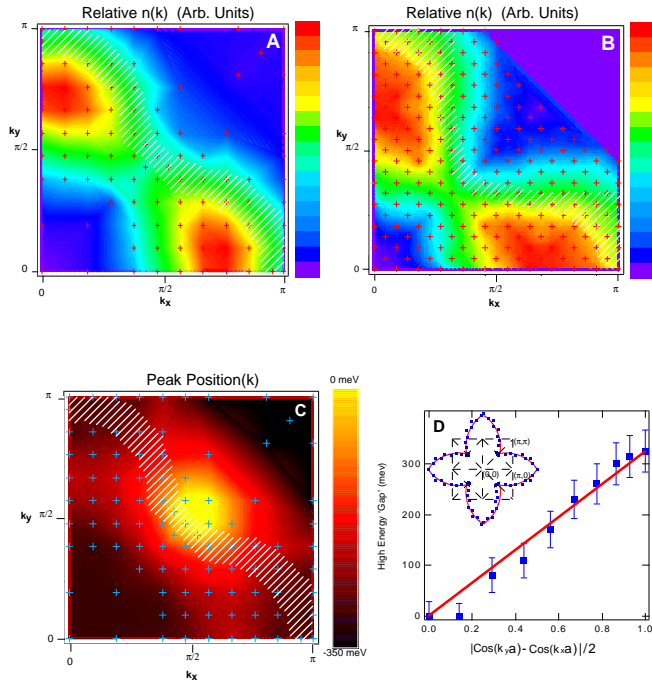


FIG. 4. Contour plot of the relative $n(k)$. (A) $n(k)$ from the spectra shown in fig. 3. The color scale on the right represent $n(k)$. The spectra were taken only in the first octant of the first Brillouin zone (crosses). The $n(k)$ plot was folded to better represent the remnant Fermi surface. Note, the $n(k)$ drops as we cross the approximate diagonal line connecting $(0, \pi)$ and $(\pi, 0)$. The hashed area represents approximately where the remnant Fermi surface exists. (B) An identical plot for an optimally doped Bi2212 sample in the normal state. (C) Contour plot of the lowest energy peak position from the spectra in fig. 3 relative to the $(\pi/2, \pi/2)$ peak. The hashed area is from (A), showing the remnant Fermi surface. The color scale on the right indicates the relative binding energy of the peak. The peak disperses isotropically away from the $(\pi/2, \pi/2)$ peak position as we move away from the $(\pi/2, \pi/2)$ point. (D) The 'gap' versus $|\cos(k_x a) - \cos(k_y a)|/2$. The straight line shows the d -wave line. The inset is a more illustrative figure of the same data as explained in the text.

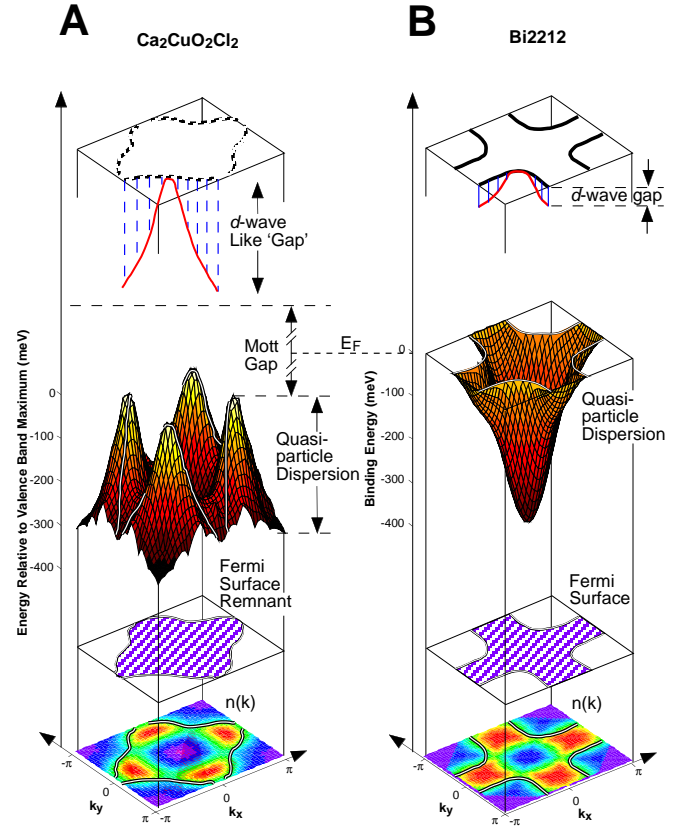


FIG. 5. An illustration showing the 2 experimental features presented in this paper on the insulator, and the similarity they show to a slightly overdoped Bi2212 sample. (A) The bottom half shows the relative $n(k)$, and above it lies the approximate remnant Fermi surface derived from it. However, there is much dispersion over the entire Brillouin zone, and the remnant Fermi surface is no longer an iso-energetic contour as can be seen by the quasiparticle dispersion (energy relative to the valence band maximum). Here the remnant Fermi surface is shown as a black and white line running over the visible portions of the dispersion contour. For clarity, a portion of the dispersion along the remnant Fermi surface is shown in the top half. Note the idea presented that the isoenergetic contour (dashed black line) is deformed by strong correlation to the observed red curve. The d -wave like 'gap' referred to in the text is the quasiparticle energy deviation from the dashed black line set at the energy of the $(\pi/2, \pi/2)$ point. The difference between this 'gap' and the Mott gap can now be seen clearly. (B) For overdoped Bi2212 , $n(k)$ defines the actual Fermi surface. The quasiparticle dispersion (binding energy) shows states filled to an isoenergetic Fermi surface. In the top panel one is reminded that below T_c , a d -wave superconducting gap opens. This is an intriguing similarity between the insulator and the metal.

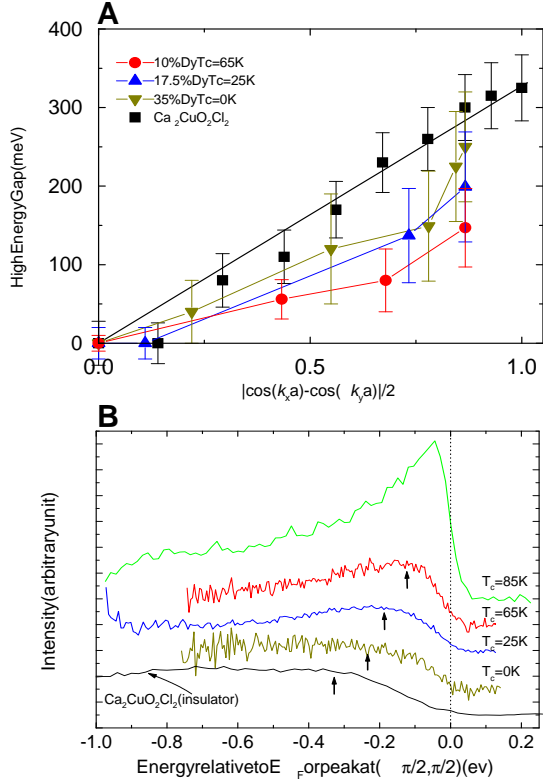


FIG. 6. (A) Combined d -wave plot of the data from $\text{Ca}_2\text{CuO}_2\text{Cl}_2$ and Bi2212 with various Dy dopings. (B) The spectra at $(\pi, 0)$, showing the evolution of the high energy pseudo gap as a function of doping, as previously stressed by Laughlin. [12]